Journal of Magnetic Resonance 286 (2018) 82–90

Contents lists available at ScienceDirect

Journal of Magnetic Resonance

journal homepage: www.elsevier.com/locate/jmr

Probing numerical Laplace inversion methods for two and three-site molecular exchange between interconnected pore structures

Emilia V. Silletta, María B. Franzoni *, Gustavo A. Monti, Rodolfo H. Acosta

Universidad Nacional de Córdoba, Facultad de Matemática, Física, Astronomía y Computación, Córdoba, Argentina
CONICET, IFEG, Córdoba, Argentina

ARTICLE INFO

Article history:
Received 7 September 2017
Revised 14 November 2017
Accepted 26 November 2017

Keywords:
NMR methods
Molecular exchange
Numerical inverse Laplace transform
Pore size distribution
Polymeric porous network

ABSTRACT

Two-dimension (2D) Nuclear Magnetic Resonance relaxometry experiments are a powerful tool extensively used to probe the interaction among different pore structures, mostly in inorganic systems. The analysis of the collected experimental data generally consists of a 2D numerical inversion of time-domain data where T_2-T_2 maps are generated. Through the years, different algorithms for the numerical inversion have been proposed. In this paper, two different algorithms for numerical inversion are tested and compared under different conditions of exchange dynamics; the method based on Butler–Reeds–Dawson (BRD) algorithm and the fast-iterative shrinkage-thresholding algorithm (FISTA) method. By constructing a theoretical model, the algorithms were tested for a two- and three-site porous media, varying the exchange rates parameters, the pore sizes and the signal to noise ratio. In order to test the methods under realistic experimental conditions, a challenging organic system was chosen. The molecular exchange rates of water confined in hierarchical porous polymeric networks were obtained, for a two- and three-site porous media. Data processed with the BRD method was found to be accurate only under certain conditions of the exchange parameters, while data processed with the FISTA method is precise for all the studied parameters, except when SNR conditions are extreme.

1. Introduction

Porous materials are spread in a great variety of systems in nature and complex technological applications. Knowledge of the fluid dynamics of a liquid imbibed in a porous medium is a central issue in most applications, where the pore size, liquid-surface interactions, and pore interconnectivity are among the main parameters that drive the fluid dynamics. Nuclear magnetic resonance (NMR) is considered today an indispensable tool for the study of porous media in many research and industrial areas such as in sedimentary rocks in oil industry [1,2], soil research [3] or cement pastes [4]. For interconnected pores, a central question concerns the migration of molecules from site to site under conditions of detailed balance.

Two-dimensional (2D) relaxation exchange NMR is a tool that is able to map diffusion of a fluid from one pore to another. In particular, T_2-T_2 correlation spectroscopy tracks changes in transverse relaxation time T_2 of molecules that change their environments during the experimental time [4–6]. The experiment consists of two Carr-Purcell-Meiboom-Gill (CPMG) [7,8] sequences encoding T_2, with a variable storage time in between during which molecules are able to exchange sites and to relax with the longitudinal relaxation time, T_1. The resulting 2D matrix contains information on relaxation in both dimensions and can be converted in a T_2-T_2 spectrum by a Numeric Laplace inversion (NLI) of the 2D data. Different approaches for the numeric inversion have been proposed and many of them use the Tikhonov regularization [9–13]. After data inversion, a T_2-T_2 map is generated whose main features are the peaks present in the diagonal which, for short storage times, reflect the number of molecules present in each environment, weighted by longitudinal relaxation. For long storage times, given that effectively an exchange process occurs, off-diagonal peaks appear. From the intensity of these peaks as a function of the storage time, exchange rates can be calculated [6,14].

The numerical inversion approach most widely used up to the moment is the data compression proposed by Venkataramanan et al. [9], using singular value decomposition of the involved kernel matrices, which uses an adaptation of Butler-Reeds-Dawson (BRD) method to solve 2D and 2.5D Fredholm integrals of the first class [15]. The interpretation of the intensity evolution of off-diagonal peaks is not straightforward, especially for systems with more than

* Corresponding author at: Universidad Nacional de Córdoba, Facultad de Matemática, Física, Astronomía y Computación, Córdoba, Argentina and CONICET, IFEG, Córdoba, Argentina.
E-mail address: franzoni@famaf.unc.edu.ar (M.B. Franzoni).

https://doi.org/10.1016/j.jmr.2017.11.016
1090-7807/

two coupled pores. Since exchange is a symmetric process, the T_2-T_2 map should be symmetric in relation to the diagonal for every storage time. However, this is not the case for many of the T_2-T_2 maps reported in the literature [4,6,16,17] and many hypotheses were made in order to explain this phenomenon. Washburn et al. [6] argued that the symmetry of the experiment was broken due to T_1 relaxation during the storage time. In a latter report, Mitchell [4] showed that the observed asymmetry was, in fact, originated during the data inversion algorithm. Additionally, the influence of the signal to noise ratio (SNR) of the experimental data on the NLI was presented by Fleury and Soualem [16], where synthetic 2D time-domain signals were generated for a two-site system. There, displacements of the position of the four peaks obtained after numerical inversion for three different values of SNR were shown. These calculations evidenced that even with a low level of the SNR, small off-diagonal peaks can be detected but their locations differ from the theoretical position while for high SNR (500), the positions are the expected ones. Another effect observed when the experiments are done with a poor SNR is the appearance of spurious peaks. Apparently, the SNR did not affect the symmetric character of the process in the sense that both off-diagonal peaks are of the same amplitude. In the same work, T_2-T_2 relaxation maps for a smectite gel at a clay fraction of 30% as a function of the storage time were presented (see Fig. 9 in Ref. [16]). In those experiments, it is clear that the non-diagonal peaks are not only deviated from the perfect square position as predicted but also their amplitudes are not the same. Recently, Song et al. argued that the typical T_2-T_2 inversion of the signal does not place the diagonal symmetry constraints in the data, and consequently allows for an asymmetrical T_2-T_2 spectrum. They introduced a different approach, showing that by analysing the time-domain 2D data in a two-site system, the exchange may be determined, preventing the presence of asymmetries [18]. The method is qualitative but it has the potential to be improved to quantify exchange and extended to systems larger than two-site. With a different strategy, d'Eurydice et al. have adjusted the experimental procedure in such a way that the exchange among different populations can be quantified without the numerical 2D inversion of the data [19]. They introduced the T_2 filtered T_2-T_2 sequence in which the first CPMG acts as a filter and the exchange rates can be calculated monitoring the 1D T_2 distributions as a function of the storage time.

Recently, Teal and Eccles [10] proposed an algorithm which does not require a matrix factorization. The idea of the algorithm is based on the fast iterative shrinkage-thresholding algorithm (FISTA) [20] but with the NMR convention, which is l_2 regularization. More recently, Zhou et al. used the FISTA algorithm for the inversion of the 2D NMR relaxometry data using l_1 regularization [21].

In the present work, two different approaches for the Numerical Laplace Inversion of the 2D data [9,10] are contrasted for a two- and three-site porous system. From a theoretical point of view, 2D synthetic signals are numerically generated, processed with the studied NLI algorithms and compared with the exact analytical solutions for different sets of parameters of the exchange dynamics. For an experimental perspective, a porous polymeric network which can be prepared with a controlled hierarchy of micro-, meso-, and macro-porous spatial domains [22] was used as a realistic model. The two algorithms were studied under different conditions, limiting values for the exchange parameters at which each of the processing algorithms begins to fail were obtained.

2. Materials and methods

In order to shed some light on the correct interpretation of the T_2-T_2 NMR data, two theoretical methods will be compared: synthetic 2D signals will be generated through numeric calculations, numerically inverted with both studied algorithms, and compared to the analytic solution of the same problem. Both theoretical results will be contrasted with the experimental data for two- and three-site porous media showing exchange among all of the reservoirs involved.

2.1. NMR measurements

The NMR pulse sequence used to acquire the T_2-T_2 signals is shown in Fig. 1. The experiment consists of three blocks; a first period encodes transverse magnetization which evolves under the influence of a CPMG pulse sequence of variable duration τ_1. A subsequent $\pi/2$ rotation stores the magnetization along with the external magnetic field axis, where diffusion takes place together with longitudinal relaxation, T_1, during a variable storage time t_s. Finally, another $\pi/2$ pulse is applied and transverse relaxation is detected by a second CPMG block of fixed duration τ_2. This sequence is repeated using a range of storage times to observe the movement of water between the different pools.

Measurements were carried out at 30 °C using a MagritekKea2 spectrometer operating at 60 MHz for protons and a Varian EM360 permanent magnet. The length of the radiofrequency pulses was set to 16 μs, the echo time t_E = 0.5 ms and 8000 echoes were acquired in the direct dimension while 32 logarithmically spaced points, from 1 to 8000 echoes, were used for the indirect dimension. The storage time was varied from 1 to 350 ms averaging 64 scans.

2.2. Two and three-site porous media: sample preparation

The study was performed using polymer beads with hierarchical pore structure corresponding to copolymers of ethylene glycol dimethacrylate and 2-hydroxyethyl methacrylate [poly(EGDMA-co-HEMA)] synthesized as previously reported [22]. Polymer networks prepared with a cross-linker content of 33 mol% of EGDMA were reported to render a system with hierarchically distributed pore sizes. The system has a porosity of 84% both in the dry state or fully saturated with water. This is an important fact as the system is used fully and partially saturated with water in this study, thus, it can be assured that the pore network is not modified. The void space sizes were previously determined by mercury porosimetry for the dry state [22] and by NMR using the Decay due to Diffusion in the Internal Field (DDIF) sequence [23] for the swollen state. Assuming a distribution of spherical pores three mean sizes were reported. The relevant parameters are listed in Table 1 [24].

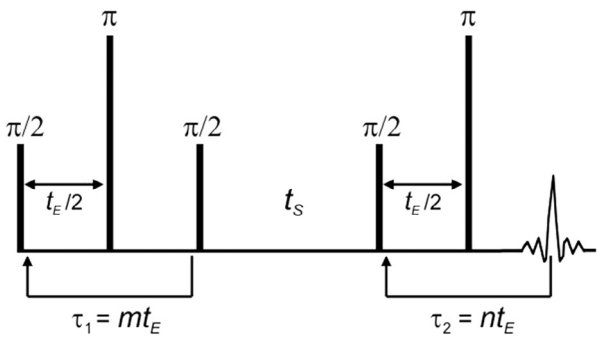

Fig. 1. Two-dimensional pulse sequence T_2-T_2 for the measurement of transverse relaxation exchange. The first CPMG encodes T_2, followed by a storage period t_s in which the magnetization is along with the z-axis and relaxes due to T_1. When finalized that period, the magnetization is turned to the plane and a second CPMG acquires the data. The 2D sequence is repeated for different storage times t_s.

Table 1
Mean pore diameter and relaxation times obtained at 60 MHz and 30 °C. The pore size values correspond to the polymeric networks fully imbibed in water. T_1 and T_2 correspond to the relaxation times of water in each of the different environments. Pore P_3 was partially saturated to 25% of its volume in order to obtain a signal low enough so as not to mask the cross-peak arising from P_1 (see Fig. 6 from Ref. [25] for the relation of relaxation times with pore-filling degree).

Site	d [μm]	T_1 [ms]	T_2 [ms]
P_1	10	75	4
P_2	36	570	40
P_3	100	1500	300

Through measurements of water evaporation kinetics, which can be discriminated within each pore by means of T_2 relaxation measurements in homogeneous fields [25], and spatially resolved by using a single-sided NMR-MOUSE® (MObile Universal Surface Explorer), it can be inferred that the system is fully interconnected. Recently, it could be demonstrated that water migration through the pores by capillary forces provides a hydrodynamic flux that maintains a constant level of water at the evaporating surface while lower pores are depleted [26]. This process is known as a funicular regime, and lasts until the continuity in the hydrodynamic connection is lost, entering to the pendular regime [27]. For the systems used in this work, the transition from a funicular to a pendular regime corresponds to a depletion of water from the larger cavities, thus defining a two-site porous system [26].

Small samples of polymer beads were immersed in a vial containing distilled water at room temperature for 24 h to reach the full swelling of the network. Samples of 75 mg weight were extracted from the vial and gently placed in a 5 mm outer diameter NMR sample tube. For this setup, the transition from a funicular to a pendular regime takes ca. 15 h at ambient pressure and temperature conditions [25]. This enables a high precision on the preparation of a system where only the smaller and intermediate pores are saturated with water (two-site system). After this time, the NMR tube was sealed leak-tight and hence the system consists of a two coupled pores polymeric network. In the same way, a tube with the saturated system was sealed after the larger pore filling degree was 25% (three-site system), to prevent that a higher signal from this pore masked the cross-peaks arising from the smaller pores. These two polymeric systems were contrasted with numerical and analytical results in order to study two- and three-pore systems.

In Fig. 2 T2-T2 maps for two- and three-site polymeric systems are shown. The two-site system can be extended to a three-site system and the exchange among pores 1 and 2 is almost unaffected, as can be inferred from the position of the four involved peaks. This is a clear benefit of the studied hierarchical polymeric system which provides the appropriate scenario to compare the exchange in the case of two and three populations, under equal environmental conditions.

2.3. Numerical Laplace inversion

In the following, we provide a short revision on how the signal collected during 2D experiments can be processed using a NLI, which is known to be an ill-conditioned procedure. The data obtained from the T_2-T_2 experiments can be expressed in the form of a 2D Fredholm integral of the first kind,

$$\mathrm{M}(\tau_1,\tau_2) = \int\int_{T_{2\min}}^{T_{2\max}} k_1(\tau_1,T_2)k_2(\tau_2,T_2)S(T_2,T_2)dT_2dT_2, \qquad (1)$$

where $\tau_1 = mt_E$ and $\tau_2 = nt_E$ (see Fig. 1). $S(T_2,T_2)$ is the unknown T_2-T_2 spectrum, M denotes the measured data, and the kernels k_1 and k_2 are given by, $k_1(\tau_1,T_2) = e^{-\tau_1/T_2}$ $k_2(\tau_2,T_2) = e^{-\tau_2/T_2}$.

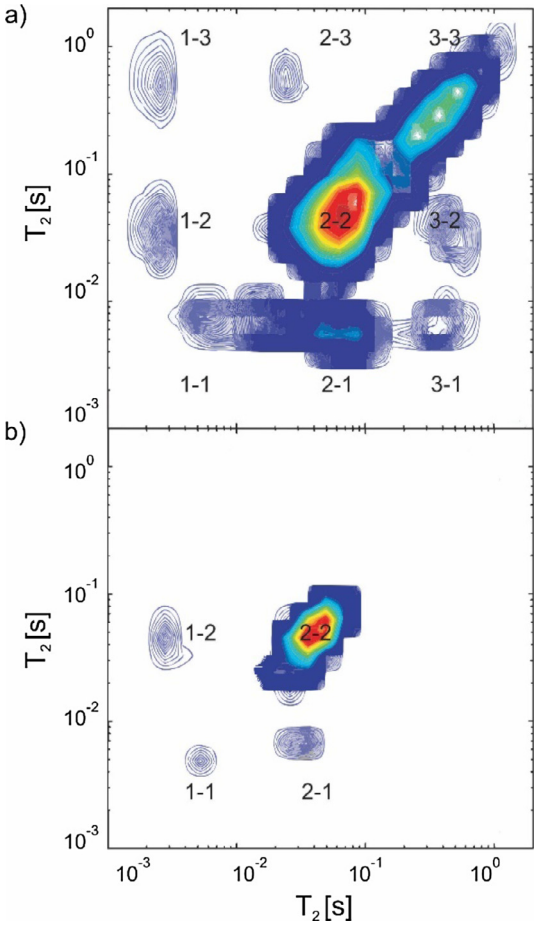

Fig. 2. T_2-T_2 maps for (a) three-site system and (b) two-site system with 150 ms of storage time. The smallest pore is called P_1, the intermediate P_2, and the biggest one P_3. The pairs of numbers represent the pores that are correlated after the 2D NLI with the BRD method. The presence of off-diagonal peaks indicates an effective exchange between every pore.

Experimental data is collected at discrete values of time and Eq. (1) is typically given as:

$$M = K_1 S K_2^{\mathrm{T}} + E,$$

where E represents white Gaussian noise, with zero mean and variance σ^2. By defining $m = \mathrm{vec(M)}$, $s = \mathrm{vec(S)}$ and $\eta = \mathrm{vec(E)}$, and $K = K_2 \otimes \mathrm{K}_1$ the equation to be solved is:

$$m = Ks + \eta. \qquad (2)$$

As the matrices K_1 and K_2 are ill-conditioned, solving Eq. (2) is a very ill-posed problem. A traditional approach to solve these problems uses Tikhonov regularization, with the solution to s given by

$$s = \arg\min_s \|m - Ks\|^2 + \alpha R(s)$$

with $\alpha > 0$ the regularization parameter and R the regularization matrix. The approach proposed by Venkataramanan et al. [9] uses singular value decomposition and after truncation of singular values, new $\tilde{K_1}$ and $\tilde{K_2}$ vectors are obtained, which drastically reduce the number of rows when compared to K_1 and K_2. After this dimension reduction, the algorithm uses an adaptation of Butler-Reeds-Dawson [15] method to solve the regularization problem. In the present work, we will refer to the BRD method when this approach is used. Relaxation maps were constructed using a 2D NLI software provided by Petrik Galvosas, from the University of Wellington, New Zealand.

The second algorithm studied in the present paper is the one proposed by Teal and Eccles [10]. This method uses a version of the FISTA algorithm [20] restricted to NMR convention, which is l_2 regularization. With this version, a faster algorithm with results comparable to the results produced by the BRD methods was obtained. The FISTA method does not require matrix factorization and iterations are performed using the kernel matrices K_1 and K_2, without the use of the much larger K matrix. This provides significant speed advantages and convergence facilities. Teal and Eccles [10] compare the l_2 regularization methods, for both simulated and measured data in terms of convergence. In this work, the algorithm provided by Paul Teal was used. The efficiency gained with the proposed FISTA algorithm allows for better resolution of the 2D maps. For the analysis shown in the following sections, maps with 32×32 pixels were constructed with the BRD method while with FISTA algorithm the maps had up to 100×100 points. Changes in the resolution using the FISTA algorithm from 32×32 to 100×100 points did not show any significant changes in the observed behaviour of the relaxation cross-peaks.

2.4. Theoretical calculations

In this section, we provide the line out for the theory of exchange among different pores within a sample studied by means of a T_2-T_2 NMR experiment. The NMR signal results from the superposition of the magnetization components $M_i(t)$ on the plane transverse to the longitudinal field:

$$s(t) = \sum_i [M_i(t) - M_i^{eq}], \tag{3}$$

where M_i^{eq} stands for the equilibrium magnetization, $M_i^{eq} = M_i^0$ for longitudinal relaxation, and $M_i^{eq} = 0$ for transversal relaxation. The evolution of the magnetization during the pulse sequence of the whole sample is collected in a vector that follows the differential equation [28]:

$$\frac{d}{dt}[\boldsymbol{M}(t) - \boldsymbol{M}^{eq}] = -(\boldsymbol{R} + \boldsymbol{K})[\boldsymbol{M}(t) - \boldsymbol{M}^{eq}], \tag{4}$$

where $\boldsymbol{R}$ is a diagonal matrix containing the relaxation rates, which are defined as $R_i^{(1)} = 1/T_i^{(1)}$ and $R_i^{(2)} = 1/T_i^{(2)}$ for a spin bearing particle i subject to longitudinal or transverse relaxation. $\boldsymbol{K}$ is the kinetic matrix that describes the exchange between different sites which, for a three-site problem can be written as

$$\boldsymbol{K} = \begin{bmatrix} k_{11} & -k_{12} & -k_{13} \\ -k_{21} & k_{22} & -k_{23} \\ -k_{31} & -k_{32} & k_{33} \end{bmatrix}, \tag{5}$$

where k_{ij} is the exchange rate between sites i and j. As $\boldsymbol{K}$ only mixes magnetization, detailed mass balance requires that a lost component must be recovered by another one, such that:

$$\boldsymbol{K}\boldsymbol{M}^{eq} = 0. \tag{6}$$

This leads to the condition $k_{11} - k_{21} - k_{31} = 0$ that is, the sum of the columns of $\boldsymbol{K}$ is zero. From the initial nine exchange constants, only four remain independent. The solution of Eq. (4) is:

$$\mathbf{M}(t) - \mathbf{M}^{eq} = \exp[-(\mathbf{R} + \mathbf{K})(t - t_0)][\mathbf{M}(t_0) - \mathbf{M}^{eq}], \tag{7}$$

where the exponential operator, known as time evolution operator, can be obtained by diagonalizing the matrix $\boldsymbol{R} + \boldsymbol{K}$. The eigenvalues of this matrix for the two-site problem are already complicated expressions [4] and for more than two pores can be analytically solved only under some particular conditions. In the present work, the equations for the three-site exchange under the detailed balance among pairs condition were analytically solved and compared to numerical results.

For the calculations, the equations here depicted are solved, either in a numerical or analytical manner for the three blocks of the T_2-T_2 experiment. The relaxation and exchange parameters in the calculations can be chosen to fit the experiments or can be known from previous experiments. After the complete evolution, a synthetic 2D signal is generated and processed in the same way as the experimental data, by inverting the data through the NLI.

As a second theoretical method, the equations are solved analytically and the magnetization as a function of the storage time is exactly obtained. The results are contrasted with the experimental and numerical ones. For the two-site case, no approximations in the dynamics need to be done and the equations can be analytically solved [4,14] and the eigenvalues for each of the three periods of evolution in the T_2-T_2 experiment can be obtained. Eq. (4) is solved considering the detailed balance, and the amplitude of the four peaks is obtained exactly. For the three-site case, the analytical solution can be obtained under some approximations, in this paper, the detailed balance among pairs is considered; this is:

$$k_{12}M_1^{eq} = k_{21}M_2^{eq}; k_{13}M_1^{eq} = k_{31}M_3^{eq}; k_{23}M_2^{eq} = k_{32}M_3^{eq} \tag{8}$$

When the detailed balance is considered, differential equation (7) can be solved by calculating the corresponding eigenvectors and eigenvalues. The analytical expressions are extremely complicated but can be easily obtained in a closed form by means of a symbolic computing environment (Maple). The validity of this approximation for the studied cases is empirically demonstrated in the following section.

Notice that the experimental and numerical results are processed with the same algorithm while the analytical results do not require data inversion. In the following section both theoretical methods will be compared for the same set of parameters and used to fit the experimental results.

3. Results and discussion

3.1. Two-site system

There are several parameters that determine an exchange process, such as the number of involved populations, the exchange rates, the initial and relative initial populations, etc. In order to test the numerical Laplace inversion under different conditions, we begin by analysing how different exchange rates influence the outcome for a two-site system resembling Fig. 2b, with initial population values $M_1^{eq} = 1; M_2^{eq} = 5$. The exchange rate parameter was varied from $k_{12} = 2 \times 10^{-4}\ ms^{-1}$ to $5 \times 10^{-2}\ ms^{-1}$ with the analogous k_{21} defined by the detailed balance condition (Eq. (8)). In each case, the synthetic 2D signal was numerically calculated and a T_2-T_2 map created using either the BRD or the FISTA algorithm. To quantify the exchange processes, the quantities A_{12} and A_{21} were obtained by evaluating the amplitude of the respective off-diagonal peak and normalized to the total system magnetization at each time. To study the influence of the inversion algorithm in the asymmetries, Fig. 3 is constructed by evaluating the asymptotic ratio A_{12}/A_{21} as a function of the exchange rate. In the case of the BRD algorithm, for all of these exchange rates, the amplitudes of the cross peaks are not equal, with ratios of the asymptotic values ranging from 0.4 for low rates to 0.9 the higher exchange rates. On the contrary, in the case of data processed with the FISTA algorithm A_{21} and A_{12} peaks are very similar for every exchange parameter tested. That is, as expected, exchange peaks on either side of the T_2-T_2 diagonal have equal intensities for all times [14].

The results in Fig. 3, show a quantitative asymmetry when data is analyzed with the BRD algorithm. In the following, for a qualitative comparison, each exchange amplitude A_{12} and A_{21} was nor-

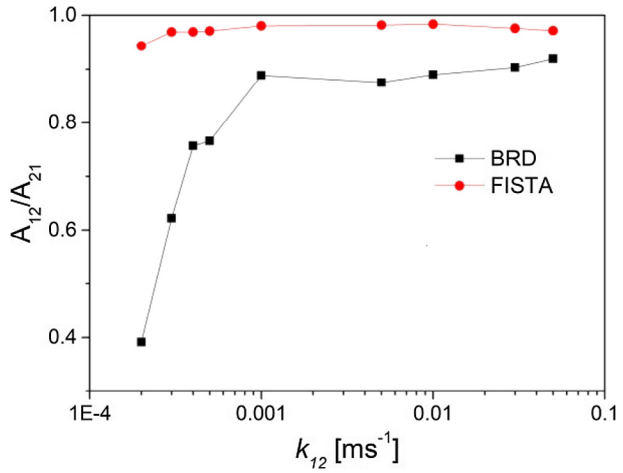

Fig. 3. Amplitude ratio of the cross-peak asymptotic amplitudes, for a simulated two-site system obtained by inversion with the BRD and FISTA methods. $M_1^{eq} = 1; M_2^{eq} = 5$. No noise addition.

malized to its maximum value and studied as a function of the storage time, t_s. In Fig. 4a and b the parameters A_{12} and A_{21} obtained with the BRD method are plotted as a function of the storage time t_s. It is clear that for low exchange rates a great asymmetry in the peak amplitudes is present and the time evolution of the numerically inverted data do not represent the system's dynamics. Notice that in those cases, neither A_{12}, A_{21} nor their average, should be used to quantify the exchange rate of a system. It can be observed, however, that for exchange rates higher than 5×10^{-3} ms^{-1} both cross-peaks describe accurately the system's time evolution, even though the amplitudes differ by 10%.

In Fig. 4c the parameters A_{12} and A_{21} obtained with the FISTA algorithm are plotted and match the analytically solved differential equation (Eq. (4)), as can be seen by comparison to Fig. 4d. From these simple calculations, it can be concluded that, even in the absence of noise, when the exchange dynamic is slow, the data processed with the BRD algorithm does not describe the system evolution. On the other hand, data processed with the FISTA algorithm is in full agreement with the analytical results for all range of exchange parameters studied here.

For the two-site porous polymeric system, both methods provide reliable information as the exchange rate of water between the pores is high enough to be described by BRD, even in the presence of noise. It must be taken into account that the total magnetization decays with the storage time, consequently, the SNR is not a constant value in the complete exchange experiment. As a reference, the SNR observed for the shortest $t_s = 30$ ms was used (SNR = 800). The normalized amplitudes A_{12} (solid circles) and A_{21} (open circles) are plotted as a function of t_s after numerical data inversion performed with both the BRD (Fig. 5a) and FISTA (Fig. 5b) algorithms. The dotted line corresponds to the analytical solution with $k_{12} = 0.03$ ms^{-1} which provides a good description of the experimental data. It can be concluded from the data that even in presence of experimental noise, the exchange rate governing the dynamics is in the safe zone for which both inversion algorithms performed in agreement with the theoretical expectations.

3.2. Three-site system

The number of involved population pools is another parameter determining the exchange dynamics. In this section, we move to the three-site system which also gives the opportunity to study simultaneously other influencing parameters such as different initial magnetization amplitudes. Van Landeghem et al. [28] have

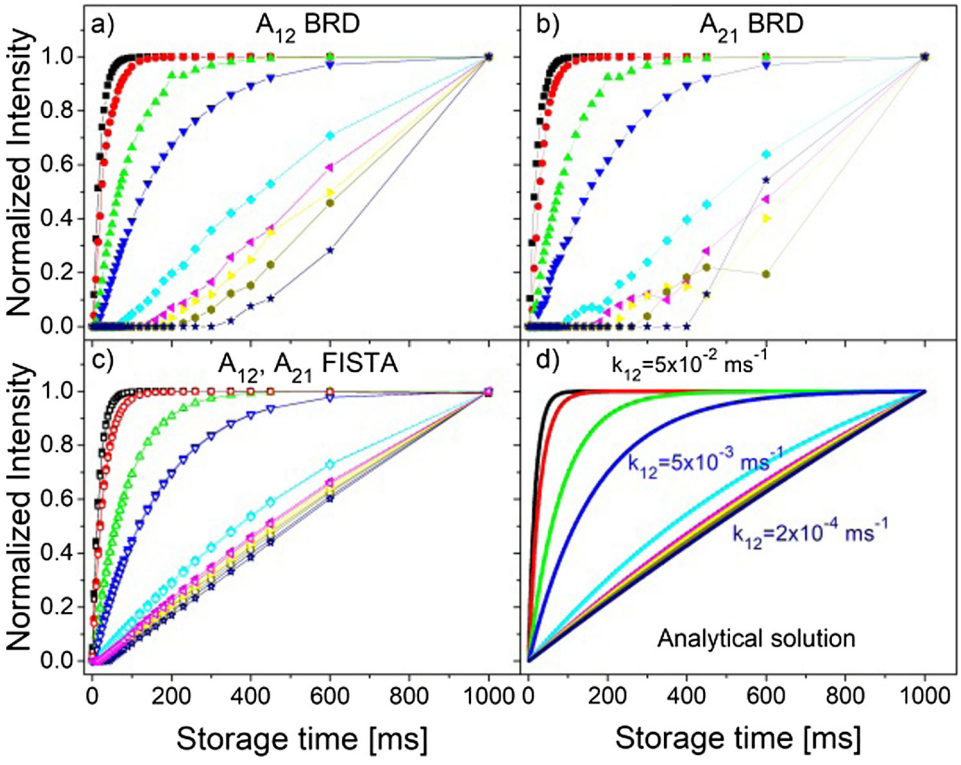

Fig. 4. Normalized intensities of the exchange peaks as a function of storage time obtained by numerical inversion of synthetic data sets. $M_1^{eq} = 1; M_2^{eq} = 5$. No noise addition. (a) A_{12} and (b) A_{21} intensities after applying the BRD algorithm. (c) Signals processed with FISTA algorithm, where close and open symbols represent A_{12} and A_{21} intensities respectively. (d) Analytical solutions for the same set of parameters without NLI.

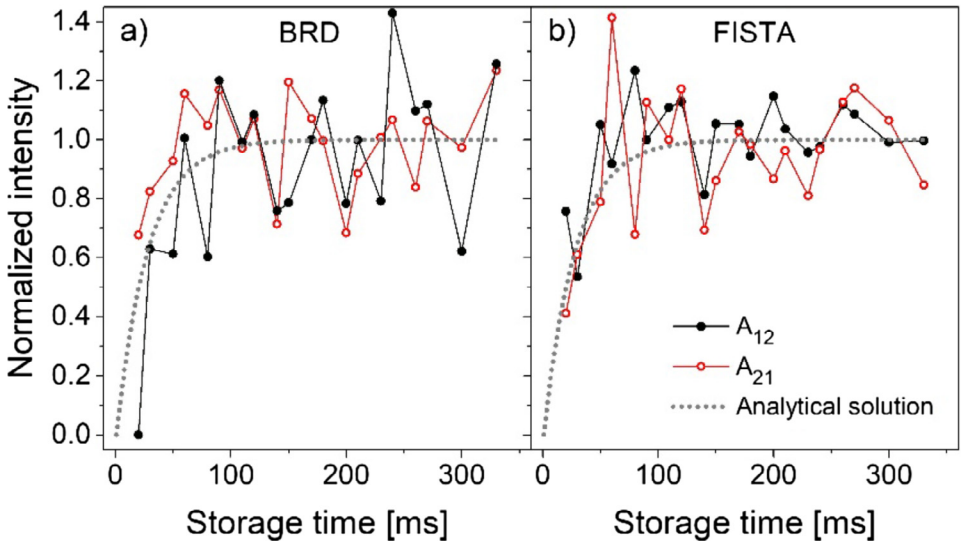

Fig. 5. Normalized experimental intensities of the exchange peaks for the two-site system using (a) BRD and (b) FISTA algorithm. Experimental data (symbols) are in good agreement with the analytical solution (dotted line) for an exchange rate $k_{12} = 0.03\ \mathrm{ms}^{-1}$. SNR = 800 for $t_s = 30$ ms.

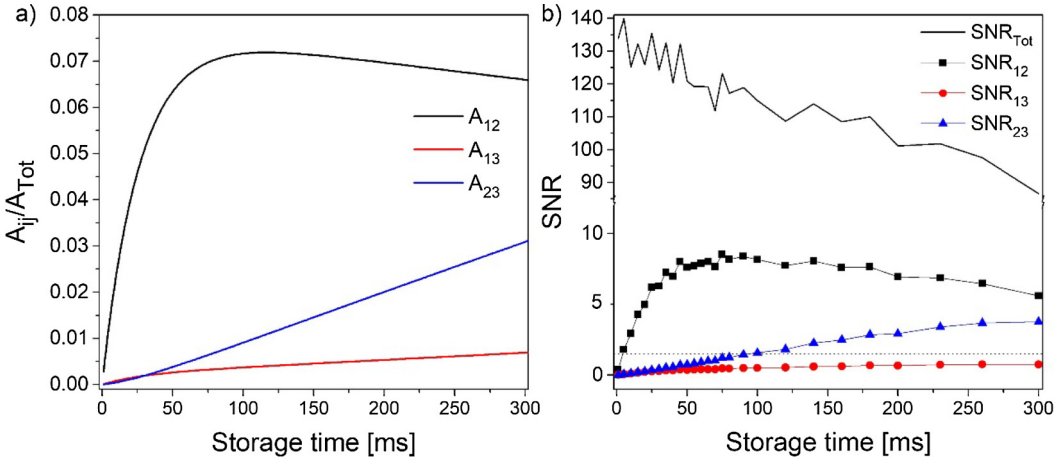

Fig. 6. (a) Theoretical calculation of the intensities of the exchange peaks for the three-site system; $M_1^{eq} = 1; M_2^{eq} = 5; M_3^{eq} = 2; k_{12} = 0.03\ \mathrm{ms}^1$; $k_{13} = 1 \times 10^3\ \mathrm{ms}^1; k_{23} = 1 \times 10^5\ \mathrm{ms}^1$. (b) Solid line, SNR estimated for the synthetic signal with noise addition, for the total signal available. In symbols, the SNR discriminated for each exchange peak. The dotted line represents the threshold value in the SNR necessary for the FISTA algorithm to obtain accurate results. Notice that S_{13} remains lower than the threshold for the whole storage time range studied.

addressed the three-site exchange problem only by numerical simulations. They argued that a source of asymmetry in experimental data can be linked to the sensitivity of the NLI algorithm to noise and baseline. However, as it was shown for the two-site system, the asymmetries appear even when the data have neither noise nor baseline when the BRD algorithm is used. In order to get quantitative information on the exchange rates, the three-site system equations were solved and the detailed balance between pairs approximation (Eq. (8)) was used. Following the same procedure used in the two-site exchange, the analytical solution for each pair of pores is compared to numerical calculations. The values used for the numerical and analytical calculations are:

$$M_1^{eq} = 1; M_2^{eq} = 5; M_3^{eq} = 2; k_{12} = 0.03\ \mathrm{ms}^1; k_{13} = 1 \times 10^3\ \mathrm{ms}^1; k_{23} = 1 \times 10^5\ \mathrm{ms}^1$$

as will be shown, these are accurate representations of the experimental data. Three pairs of exchange peaks are identified in the 2D maps shown in Fig. 2a. The analytical equation (4) is solved under the approximation of Eq. (8) and following the procedure presented for the two sites case by Monteilhet [4], the magnetization amplitude corresponding to the diagonal peaks (A_{11}, A_{22}, A_{33}) and to the exchange peaks (A_{12}, A_{13}, A_{23}) can be calculated. Fig. 6a shows the amplitude of the exchange peaks, normalized to the total magnetization amplitude $A_{Tot}(t_s) = \sum_{i,j} A_{ij}(t_s)$ at each time. As the magnetization fraction assigned to the second population M_2 is the largest, the associated quantities A_{12} and A_{23} show higher intensities. The data corresponding to exchange between the smallest and largest pores (A_{13}) present a much lower intensity due to both, lower M_1 and slower exchange rate.

Synthetic signals were constructed in order to compare the analytical results to those obtained after signal processing with ILT. Two sets of synthetic signals were numerically generated, one without noise addition and a second with noise. In Fig. 6b the SNR relationship for the synthetic 2D magnetization is shown for a SNR = 120 corresponding to the lowest exchange time. As expected the SNR decays with the storage time due to relaxation. A great advantage in the combination of analytical and synthetic

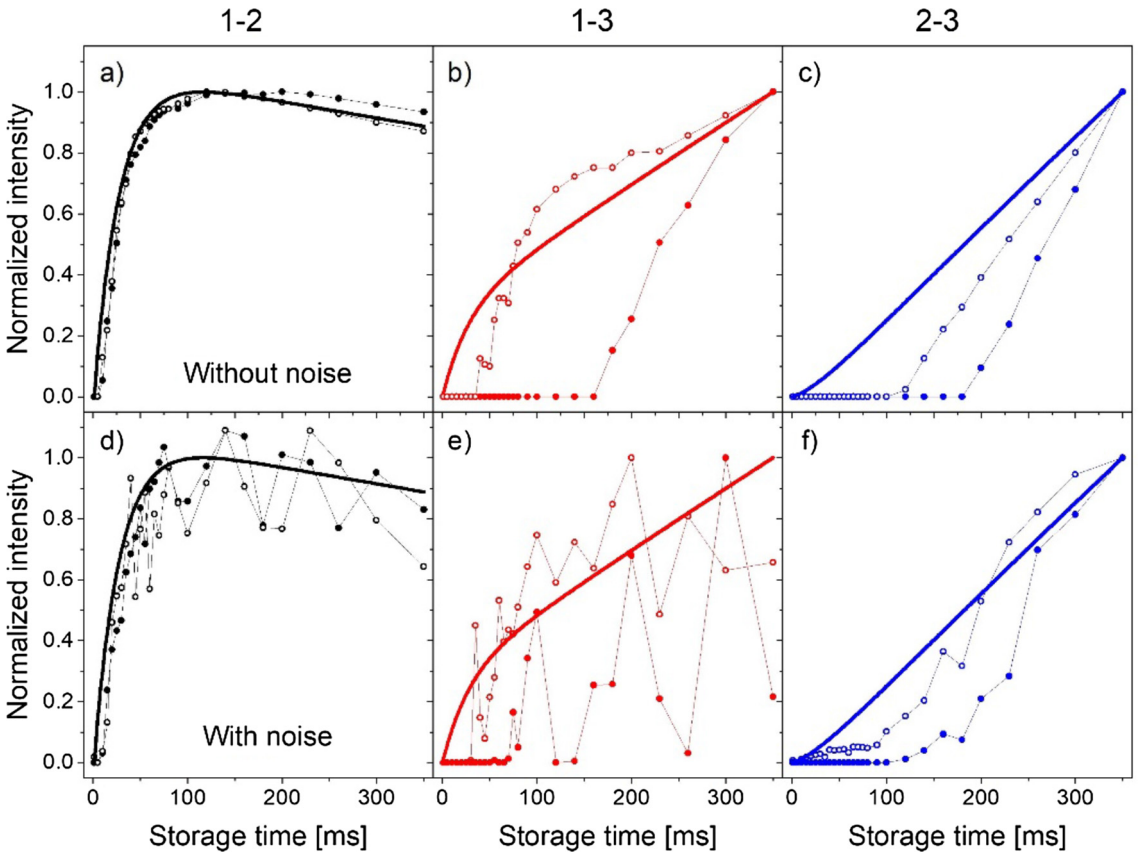

Fig. 7. Numerical calculation intensities of the off-diagonal peaks obtained with the BRD algorithm (symbols) compared with the analytical solution (color lines) for (a) 1–2, (b) 1–3 and (c) 2–3 pairs without noise. (d–f) Synthetic data with noise addition. Every data set is normalized to its own maximum value for visualization purposes. All of the solid symbols represent the data from one side to the diagonal, while the open symbols represent the other side, see Fig. 2. (For interpretation of the references to colour in this figure legend, the reader is referred to the web version of this article.)

data is that the individual contributions of each cross-peak can be analyzed without the use of a numerical inversion. In this way, an estimate of the SNR for the time domain contributions can be determined. As SNR is defined as the ratio between the initial data in the 2D data set to the RMS noise and using the fact that the magnetization at each t_s is the addition of the nine contributions A_{ij}, [4], an individual SNR_{ij} can be defined for each population as $A_{ij}/\sqrt{\overline{\sigma^2}}$. For instance, in Fig. 6b SNR = 115 for the total magnetization at t_s = 100 ms while the $SNR_{12} = 8$, $SNR_{23} = 1.5$ and $SNR_{13} = 0.5$.

In Fig. 7a–c the numerical calculation intensities after processing with the BRD method is contrasted with the analytical data. For comparison purposes, every data set is normalized to its maximum. In Fig. 7a the exchange peaks A_{12} (solid circles) and A_{21} (open circles) show good agreement with the analytical data. However, as in the two-site case, when the exchange parameter becomes smaller, an asymmetry in the amplitude of the paired exchange peaks appears, leading to an incorrect description of the system time evolution. It can be seen that A_{13} remains zero until t_s = 160 ms (solid circles in Fig. 7b), while A_{31} starts growing at a lower value of t_s = 50 ms (open circles). Data for the 3–2 cross-peak A_{32} (open circles in Fig. 7c) starts growing after a storage time of 100 ms, while a storage time of 200 ms elapses before A_{23} (solid circles) is observable. Noticeably, neither of the off-diagonal peaks obtained through BRD numerical inversion reflects the true behaviour for the 1–3 and 2–3 pairs due to the slow exchange rate. Fig. 7d–f shows the inversion of the synthetic data with noise addition (Fig. 6b). As expected, the most affected signals are those corresponding to exchange between pores 1 and 3, due to its lower intensity. According to Fig. 6b the SNR_{13} is always lower than 0.6.

On the other hand, when the data are processed with the FISTA algorithm, the results for the exchange peaks provide a better representation of the analytical solutions, as shown in Fig. 8. For data without noise addition (Fig. 8a–c), the numerical inversion slightly fails to describe the data only in the case of A_{13}, where the associated magnetization is very small. Fig. 8d–f shows the synthetic data with noise addition processed with the FISTA algorithm. The behaviour obtained for the pair 1–2 is still in good agreement with the analytical result. Still, accurate information on the evolution of the 1–3 pair could not be obtained, presumably due to the low SNR_{13}. The most interesting behaviour is observed in Fig. 8f, in the case of the 2–3 peak. Here the SNR_{23} increases with the storage time and the results describe the data evolution for storage times larger than t_s = 100 ms. From these observations, a threshold value in the SNR necessary for the FISTA algorithm to obtain accurate results can be estimated to be approximately 1.5 (dotted line in Fig. 6b), which in principle is independent of the exchange rate.

As in the two-site system, a realistic case is tested by using the polymeric network described in the sample preparation section; care was taken in order to fill the larger pore to a 25% degree to prevent the masking of the smallest pore signal. For the shortest storage time, a SNR = 900 was estimated for the total magnetization at t_s = 30 ms. In Fig. 9a–c, the amplitude of each of the six exchange peaks obtained after numerical inversion with the BRD algorithm is shown as a function of t_s. It is clear that in the case of 1–3 and 2–3 pairs, data is corrupted by the process of numerical inversion. It is worth noting that the rate of exchange in the 1–2 pair is very similar as the one in the two-site system, reflecting the fact that the pore size distribution of the polymer matrix is

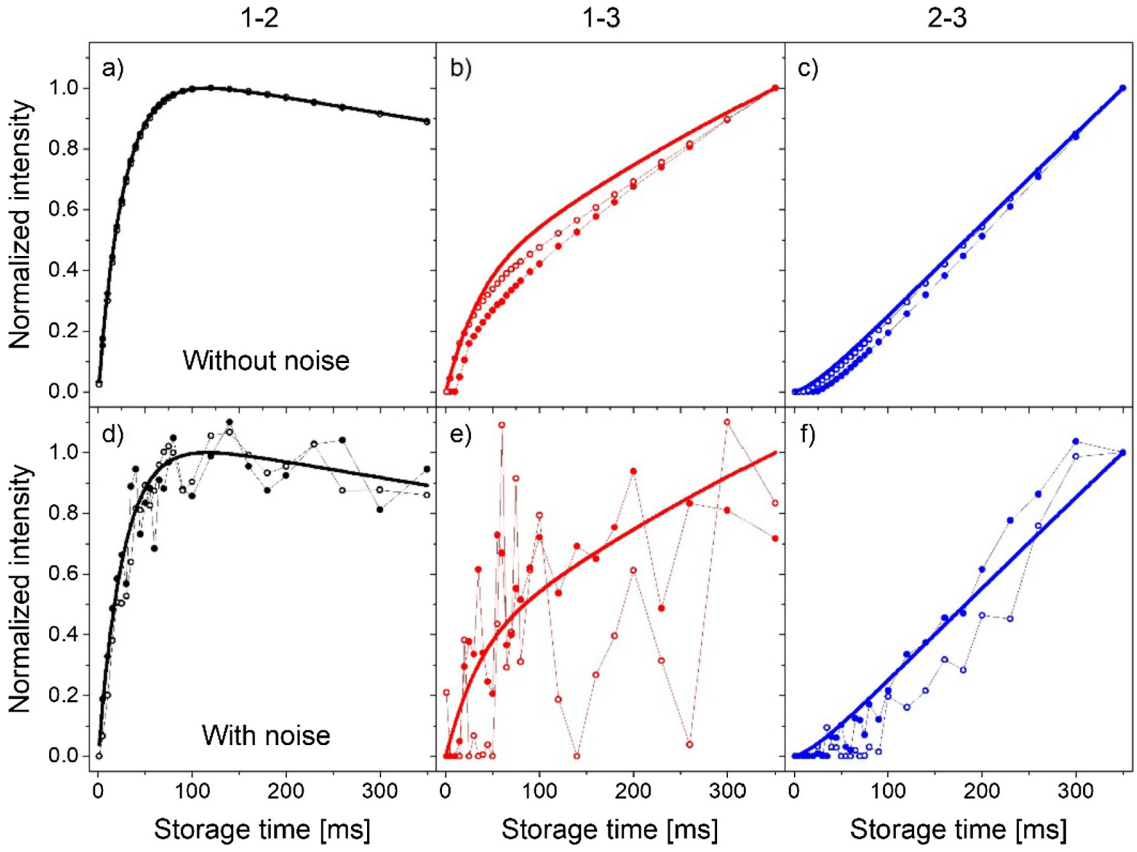

Fig. 8. Numerical calculation intensities of the off-diagonal peaks obtained with the FISTA algorithm (symbols) compared with the analytical solution (color lines) for (a) 1–2, (b) 1–3 and (c) 2–3 pairs without the addition of noise. (d–f) Synthetic signal with noise addition. Every data set is normalized to its own maximum value for visualization purposes. All of the solid symbols represent the data from one side to the diagonal, while the open symbols the opposite side, see Fig. 2. (For interpretation of the references to colour in this figure legend, the reader is referred to the web version of this article.)

not affected by the evaporation of water from the larger cavities. As in the simulated data, the exchange among the 1–3 and 2–3 pairs are not feasible to be fitted to an analytical solution. A_{13} and A_{31} evolve differently and are not observable for short storage times (see Fig. 9b). The behaviour is similar to the numerical results presented in Fig. 7b. The asymmetry among A_{23} and A_{32} is very evident in the T_2-T_2 maps; A_{23} is not visible until the very long storage times are reached, Fig. 9c.

The results are different when the FISTA algorithm is used for the NLI, see Fig. 9d–f. There is no evidence of asymmetries in the exchange peak amplitudes, in agreement with the theoretical results. When comparing the results reported in Fig. 9c and f it becomes evident how the FISTA algorithm performs better than the BRD algorithm for slower exchange rates without the creation of spurious asymmetries due to data processing. In this case when the processed data is used to estimate each pair SNR the values $SNR_{12} = 6.7$, $SNR_{23} = 1.6$ and $SNR_{13} = 0.03$ for $t_s = 100$ ms are obtained. The FISTA algorithm is unable to describe the 1–3 exchange, Fig. 9e. As occurred when noise was added to the calculations, the SNR_{13} is lower than the minimum SNR necessary for the FISTA to be accurate.

The 2D relaxation experiments studied here are commonly applied in the inorganic system, as rocks, cement, etc. In this paper, we show that even in a complex organic system, where process as swelling can take place which induces changes in the pore structure, it is possible to measure the molecular exchange rates. The exchange rates give information about the connectivity among different environments and can be used to elucidate the system tortuosity. The rates were estimated for the three different cavity pools, obtaining the values $\boldsymbol{k}_{12} = 0.03\ \mathrm{ms}^{-1}; \boldsymbol{k}_{23} = 1 \times 10^{-5}\ \mathrm{ms}^{-1}$. Due to its extremely low SNR value the exchange rate $\boldsymbol{k}_{13}$ can not be accurately determined. These results suggest that the exchange dynamics with the smallest pore is the most efficient which is in total agreement with the hierarchical pore structure observed previously by SEM [22]. This is a confirmation of the previously reported pore distribution in these hierarchical porous media [25]. There small pores (P_1) belong to a population corresponding to the polymer mesh, accessible mainly through the surface of the polymer beads. The remaining cavities are due to the agglomeration of the beads. Water confined in the larger pores, corresponding to P_3, must travel longer distances in order to exchange with water molecules confined in superficial pores (P_1), and even longer times to exchange with connected, intermediate cavities (P_2).

4. Conclusions

We presented an analysis of the performance of two different methods to carry out the numerical inversion of T_2-T_2 relaxation data: the well-established BRD method and the recently introduced FISTA algorithm. The two- and three-site exchange was analyzed; for the two-site exchange problem both methods perform comparably for the fast exchange rates and high SNR tested values. We observed that FISTA outperforms BRD for low exchange rates, as BRD presents asymmetries in the cross-peak amplitudes for rates below $1 \times 10^{-3}\ \mathrm{ms}^{-1}$ while FISTA provides an accurate description of the exchange peaks intensity evolution. In the case

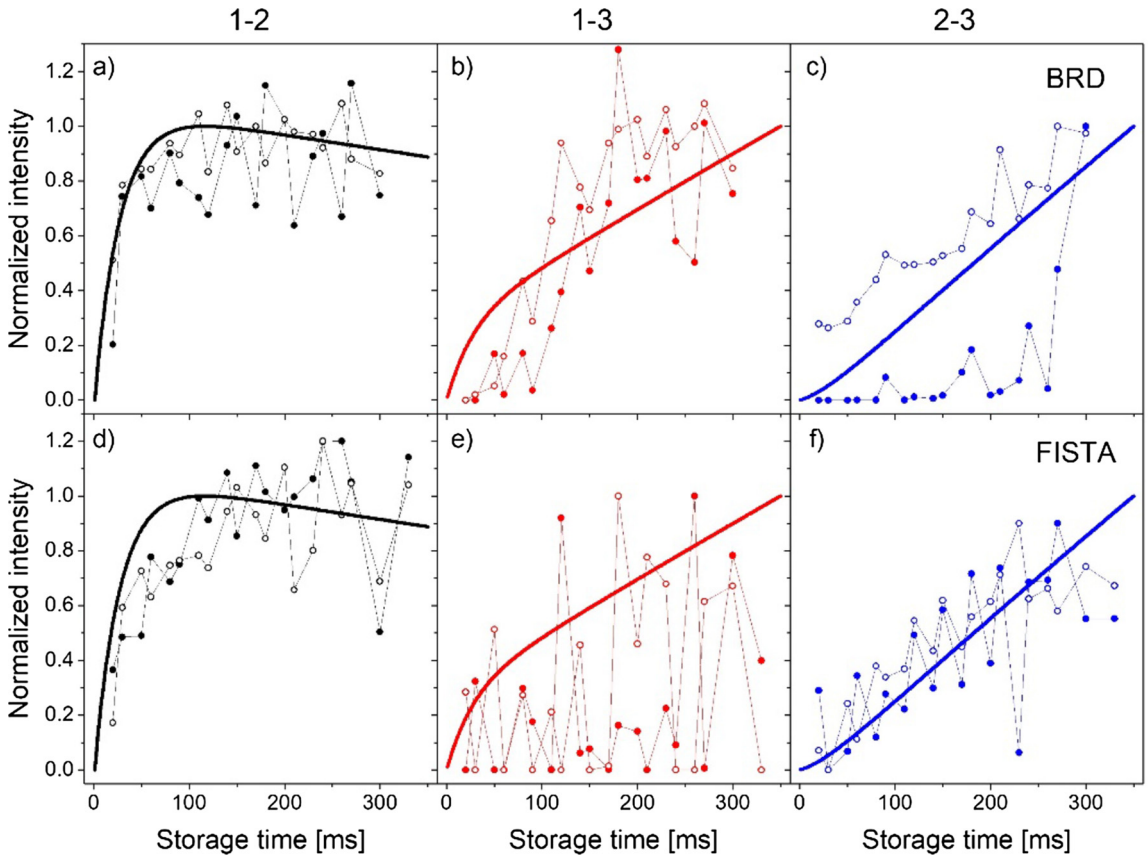

Fig. 9. Analytical solution (color line) compared with experimental intensities (symbols) of the off-diagonal peaks obtained with the BRD algorithm for (a) 1–2, (b) 1–3 and (c) 2–3 pairs and with the FISTA algorithm for (d) 1–2, (e) 1–3 and (f) 2–3 pairs. The analytical solution reproduces perfectly the 1–2 exchange process obtained with both numerical algorithms while the 2–3 pair behaviour is reproduced only when FISTA is used. The 1–3 exchange process is in any case inadequate to be analytically fitted. SNR = 900 for t_s = 30 ms. (For interpretation of the references to colour in this figure legend, the reader is referred to the web version of this article.)

of three-sites, synthetic data generated with values similar to those observed in a water-saturated porous polymer matrix were used. Additionally, a threshold value in the SNR was observed for the pool with the lowest signal intensity. The exchange rates for two pairs of sites, 12 and 23 in the water saturated porous polymer matrix could be clearly identified. However, the signal intensity corresponding to the third exchange rate is below the SNR threshold in the whole range studied. This is a powerful tool in order to tailor functional properties in these types of materials.

In summary, the FISTA algorithm appears to be a very suitable tool for the discrimination of relaxation times in 2D NMR experiments due to its stability upon low exchange rates, low SNR requirements and the possibility to reconstruct a larger number of points due to its low computational cost.

Acknowledgments

We thank Cesar Gomez and Miriam Strumia for sample preparation. We would like to acknowledge the financial support received from CONICET, ANPCyT, and SeCyT-UNC.

References

[1] Y.-Q. Song, J. Magn. Reson. 229 (2013) 12.
[2] R.L. Kleinberg, W.E. Kenyon, P.P. Mitra, J. Magn. Reson. Ser. A 108 (1994) 206.
[3] L.R. Stingaciu, A. Pohlmeier, P. Blümler, L. Weihermüller, D. van Dusschoten, S. Stapf, H. Vereecken, Water Resour. Res. 45 (2009) W08412.
[4] L. Monteilhet, J.P. Korb, J. Mitchell, P.J. McDonald, Phys. Rev. E Stat. Nonlinear, Soft Matter Phys. 74 (2006) 1.
[5] J.H. Lee, C. Labadie, C.S. Springer, G.S. Harbison, J. Am. Chem. Soc. 115 (1993) 7761.
[6] K.E. Washburn, P.T. Callaghan, Phys. Rev. Lett. 97 (2006) 25.
[7] H.Y. Carr, E.M. Purcell, Phys. Rev. 94 (1954) 630.
[8] S. Meiboom, D. Gill, Rev. Sci. Instrum. 29 (1958) 688.
[9] L. Venkataramanan, Y.-Q. Song, M.D. Hurlimann, IEEE Trans. Signal Process. 50 (2002) 1017.
[10] P.D. Teal, C. Eccles, Inverse Probl. 31 (2015) 45010.
[11] P.D. Teal, Diffus. Fundam. 22 (2014).
[12] D. Medellín, V.R. Ravi, C. Torres-Verdín, J. Magn. Reson. 269 (2016) 24.
[13] E. Chouzenoux, S. Moussaoui, J. Idier, F. Mariette, in ICASSP, IEEE Int. Conf. Acoust. Speech Signal Process. Proc., 2013, pp. 8747–8750.
[14] J. Mitchell, J.D. Griffith, J.H.P. Collins, A.J. Sederman, L.F. Gladden, M.L. Johns, J. Chem. Phys. 127 (2007) 234701.
[15] J.P. Butler, J.A. Reeds, S.V. Dawson, SIAM J. Numer. Anal. 18 (1981) 381.
[16] M. Fleury, J. Soualem, J. Colloid Interface Sci. 336 (2009) 250.
[17] P.J. McDonald, J.-P. Korb, J. Mitchell, L. Monteilhet, Phys. Rev. E. Stat. Nonlin. Soft Matter Phys. 72 (2005) 11409.
[18] R. Song, Y.-Q. Song, M. Vembusubramanian, J.L. Paulsen, J. Magn. Reson. 265 (2016) 164.
[19] M.N. d'Eurydice, E.T. Montrazi, C.A. Fortulan, T.J. Bonagamba, J. Chem. Phys. 144 (2016) 204201.
[20] A. Beck, M. Teboulle, SIAM J. Imaging Sci. 2 (2009) 183.
[21] X. Zhou, G. Su, L. Wang, S. Nie, X. Ge, J. Magn. Reson. 275 (2016) 46.
[22] C.G. Gomez, G. Pastrana, D. Serrano, E. Zuzek, M.A. Villar, M.C. Strumia, Polym. (United Kingdom) 53 (2012) 2949.
[23] Y.-Q. Song, S.G. Ryu, P.N. Sen, Nature 406 (2000) 178.
[24] E.V. Silletta, M.I. Velasco, C.G. Gomez, M.C. Strumia, S. Stapf, C. Mattea, G.A. Monti, R.H. Acosta, Langmuir 32 (2016) 7427.
[25] E.V. Silletta, M.I. Velasco, C.G. Gómez, R.H. Acosta, M.C. Strumia, G.A. Monti, Langmuir 30 (2014) 4129.
[26] M.I. Velasco, E.V. Silletta, C.G. Gomez, M.C. Strumia, S. Stapf, G.A. Monti, C. Mattea, R.H. Acosta, Langmuir 32 (2016) 2067.
[27] M. Kaviany, M. Mittal, Int. J. Heat Mass Transf. 30 (1987) 1407.
[28] M. Van Landeghem, A. Haber, J.-B. D'espinose De Lacaillerie, B. Blümich, Concepts Magn. Reson. Part A 36A (2010) 153.